Triangle Centers Relative to Their Cevian, Circumcevian, and Pedal Triangles

Ismail Hammoudeh

September 2026

Abstract

For a triangle center $P = X_i(ABC)$, we ask whether the same Euclidean point is classified as X_j relative to the cevian, circumcevian, or pedal triangle of P. Circumcevian–pedal similarity and its isogonal transfer principle are classical; we give a self-contained coordinate proof and use them as the organizing mechanism. The algebraic contribution is an explicit branch refinement for the classical family F_λ: under the positive-area convention, the target parameter is $-\lambda$ when the source is inside the circumcircle and λ when it is outside. This gives a general near-equilateral obstruction to unrestricted fixed-point claims. Affine covariance of symmetric polynomials proves the fixed relations for X_{67371} and X_{9181}. Classical relations involving the Steiner-inellipse foci and X_{187} are recovered by intrinsic proofs.

Using a local snapshot of the *Encyclopedia of Triangle Centers* (ETC) contiguous through X_{72807}, we enumerate every diagonal index and the two directed off-diagonal strips $\min(i, j) \leq 1000$. The census distinguishes exact identities, branch-dependent relations, numerical candidates, and unavailable evaluations. An audit corrects an acute-seed cache fallback, and additional high-precision tests approach special shapes systematically. The accompanying supplement contains the fixed data snapshot, readable formulas, source programs, ordered test triangles, residuals, and a final status table.

Keywords. triangle center; cevian triangle; circumcevian triangle; pedal triangle; experimental geometry; Encyclopedia of Triangle Centers.

1 The geometric question

Let ABC be a labelled, nondegenerate scalene triangle and let P be a finite point distinct from the vertices. Denote by

- $\mathcal{T}_1(P) = A_1B_1C_1$ the cevian triangle, with $A_1 = AP \cap BC$ and cyclically;
- $\mathcal{T}_2(P) = A_2B_2C_2$ the circumcevian triangle, where A_2 is the second intersection of AP with the circumcircle and cyclically;
- $\mathcal{T}_3(P) = A_3B_3C_3$ the pedal triangle, whose vertices are the perpendicular projections of P on BC, CA, AB.

Only noncollinear derived triples are admitted. We write

$$\mathcal{C}_k(i, j; ABC) : \qquad X_i(ABC) = X_j\big(\mathcal{T}_k(X_i(ABC))\big). \tag{1}$$

Thus $M_k : X_i \mapsto X_j$ records a reclassification of the *same Euclidean point in the ambient plane*; it is not an ordinary point map. The case $i = j$ is called a fixed-point candidate.

An instance of (1) is *admissible* if the source defines a finite real point, the required traces are finite, the derived vertices are distinct and noncollinear, and the target defines a finite real point on its specified ETC branch. A zero homogeneous triple is undefined; it is not a point at infinity. Common rational factors are cancelled before interpreting a formula, but no continuation of a selected algebraic root is imposed unless stated. An unrestricted identity means equality at every admissible instance of its stated real domain, not existence on every triangle.

Figure 1 summarizes the three changes of reference triangle. It is schematic rather than metrically exact.

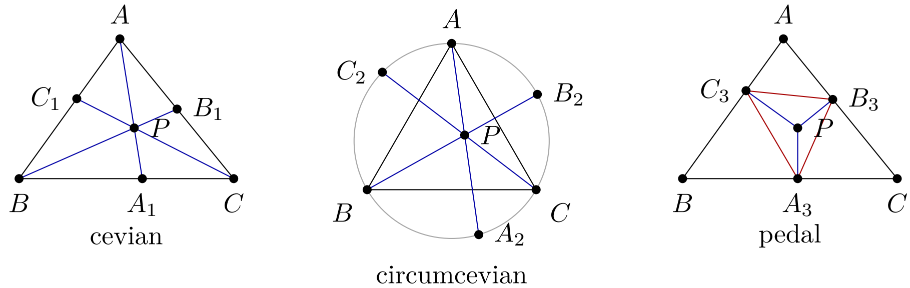

Figure 1: The three derived reference triangles in (1).

If P is on the circumcircle, $\mathcal{T}_2(P)$ collapses to P, P, P, while $\mathcal{T}_3(P)$ is collinear by the Simson theorem. Neither configuration admits an ETC target center. Selected-root definitions may also change branch as the triangle shape or its labelling changes. These facts motivate the degeneracy checks and multiple-shape audits below.

2 Classical transfer principle and exact construction

Let $P = (u : v : w)$ in barycentric coordinates of ABC, with side lengths $a = BC$, $b = CA$, $c = AB$. The cevian traces are

$$A_1 = (0 : v : w), \qquad B_1 = (u : 0 : w), \qquad C_1 = (u : v : 0).$$

The circumcircle has barycentric equation

$$a^2yz + b^2zx + c^2xy = 0.$$

Intersecting this equation with AP and removing the known root A gives

$$A_2 = (a^2vw : -v(b^2w + c^2v) : -w(b^2w + c^2v)), \tag{2}$$

with B_2, C_2 obtained cyclically. The implementation constructs all three derived triangles independently in Cartesian coordinates; equation (2) is an exact audit of the line-circle calculation.

The circumcevian and pedal problems are not independent. The following theorem provides the algebraic bridge between them.

Theorem 1 (Circumcevian–pedal isogonal transfer)**.** *Let $P = (u : v : w)$ be admissible, with $uvw(u + v + w) \neq 0$, and suppose that $\mathcal{T}_2(P)$ and $\mathcal{T}_3(P)$ are nondegenerate. Under the correspondence $A_2 \leftrightarrow A_3$, $B_2 \leftrightarrow B_3$, $C_2 \leftrightarrow C_3$, the two derived triangles have proportional corresponding squared side lengths. Moreover, the barycentric coordinate triples of the same point P in these triangles are isogonal conjugates. Consequently, for every side-defined center function X_j on a consistent branch,*

$$P = X_j(\mathcal{T}_2(P)) \quad \Longleftrightarrow \quad P = \iota(X_j)(\mathcal{T}_3(P)). \tag{3}$$

Proof. Put $A = a^2$, $B = b^2$, $C = c^2$ and $t = u + v + w$. Let R_A, R_B, R_C denote the three raw triples supplied by (2), and let s_A, s_B, s_C be their coordinate sums. Direct multiplication gives

$$uR_A + vR_B + wR_C = -(Avw + Bwu + Cuv)(u, v, w).$$

Since $A_2 = R_A/s_A$ and cyclically, the coordinates of P relative to its circumcevian triangle are therefore

$$P_{\mathcal{T}_2} = (us_A : vs_B : ws_C). \tag{4}$$

The barycentric distance formula also gives

$$PA^2 = -\frac{s_A}{t^2}, \qquad PB^2 = -\frac{s_B}{t^2}, \qquad PC^2 = -\frac{s_C}{t^2}.$$

Thus (4) may be written

$$P_{\mathcal{T}_2} = (uPA^2 : vPB^2 : wPC^2). \tag{5}$$

For comparison, the foot on BC is

$$A_3 = \frac{1}{2At}(0,\ u(A + B - C) + 2Av,\ u(A + C - B) + 2Aw),$$

with the other feet obtained cyclically. Inverting this affine matrix gives the particularly simple triple

$$P_{\mathcal{T}_3} = \left(\frac{A}{u} : \frac{B}{v} : \frac{C}{w}\right). \tag{6}$$

Let $a_2 = B_2C_2$, $a_3 = B_3C_3$, let $\mathcal{R}$ be the circumradius of ABC, and let Π_P be the signed power of P with respect to its circumcircle. The projection formula and the power-of-a-point theorem give

$$a_3^2 = \frac{a^2PA^2}{4\mathcal{R}^2}, \qquad a_2^2 = \frac{\Pi_P^2 a^2}{PB^2PC^2}.$$

Hence

$$\frac{a_2^2}{a_3^2} = \frac{4\mathcal{R}^2\Pi_P^2}{PA^2PB^2PC^2},$$

and the same factor occurs cyclically. The corresponding side triples are therefore proportional. Isogonal conjugation of (5) inside $A_2B_2C_2$ yields

$$\left(\frac{a_2^2}{uPA^2} : \frac{b_2^2}{vPB^2} : \frac{c_2^2}{wPC^2}\right) \sim \left(\frac{A}{u} : \frac{B}{v} : \frac{C}{w}\right),$$

which is exactly (6). This proves the assertion. □

3 Relation to previous circumcevian theory

The similarity of the circumcevian and pedal triangles under the natural vertex correspondence is classical; it appears in Kimberling's treatment of central triangles [2]. Stothers gave the corresponding coordinate transfer theorem and tables of circumcevian classes [3, 4]. In particular, those tables already contain the reciprocal centroid–Steiner-focus class, the invariant centers X_3, X_6, X_{187}, the class $X_{36} \leftrightarrow X_{186}$, and the one-parameter extraversion class

$$\{Q(\phi), Q(-\phi)\}, \qquad Q(\phi) = (\sin A \sin(A + \phi) : \sin B \sin(B + \phi) : \sin C \sin(C + \phi)).$$

Up to a projective scalar this is the present F_λ family with $\lambda = -\cot\phi$. Gibert's related tables also organize centers with trilinears of the form $\tan(A+t)$ and associated Brocard-axis families [5].

Accordingly, Theorem 1, the Steiner-focus result, and the X_{187} relations below are included as self-contained recoveries and as checks on notation. The contribution developed here is more specific: it distinguishes the signed, oriented identity from the usual positive-Heron convention, gives an exact formula for the branch change, uses it to disprove apparent global fixed points, proves the high-index fixed point X_{67371}, and audits a modern ETC snapshot far beyond the classical tables.

4 The exact F_λ family and its branch locus

4.1 The oriented parameter-reversal law

Put

$$H = \sqrt{(a+b-c)(a-b+c)(-a+b+c)(a+b+c)} = 4[ABC]$$

and

$$D_a = a^2 - b^2 - c^2, \qquad D_b = b^2 - c^2 - a^2, \qquad D_c = c^2 - a^2 - b^2.$$

Define

$$F_\lambda = \big(a^2(D_a + \lambda H) : b^2(D_b + \lambda H) : c^2(D_c + \lambda H)\big). \tag{7}$$

Its trilinears are

$$(-\cos A + \lambda \sin A : -\cos B + \lambda \sin B : -\cos C + \lambda \sin C).$$

In the oriented calculations choose a counterclockwise realization of ABC, so $H = 2\det(B - A, C - A) > 0$. For a derived labelled triangle $T = UVW$, write $H_T^{\mathrm{or}} = 2\det(V - U, W - U)$, and use a superscript "or" when this signed radical replaces the positive Heron radical. For an arbitrary realization, multiply the derived determinant by $\operatorname{sgn}\det(B - A, C - A)$ instead. Thus orientation is relative to the source; the positive-Heron statements below are independent of the realization.

Theorem 2 (Circumcevian parameter reversal)**.** *On the generic nondegenerate domain,*

$$F_\lambda(ABC) = F^{\mathrm{or}}_{-\lambda}(\mathcal{T}_2(F_\lambda(ABC))). \tag{8}$$

The identity extends after cancellation wherever both sides remain defined. The exceptional loci include $3\lambda^2 = 1$ and the vanishing factors displayed in the proof.

Proof. Set $A = a^2$, $B = b^2$, $C = c^2$, $S = A + B + C$; then

$$H^2 = 2AB + 2BC + 2CA - A^2 - B^2 - C^2, \qquad D_a = 2A - S.$$

Define cyclically

$$q_a = (3\lambda^2 - 1)A - 2\lambda^2 S + 2\lambda H, \qquad Q = (3\lambda^2 + 1)H - 2\lambda S. \tag{9}$$

Substitution of $u = A(D_a + \lambda H)$ and its cyclic companions into (2) shows that the coordinate sums of the raw circumcevian triples are

$$s_A = BCH^2 q_a, \qquad s_B = CAH^2 q_b, \qquad s_C = ABH^2 q_c.$$

By (4), the original point relative to its circumcevian triangle therefore has coordinates

$$\big((D_a + \lambda H)q_a : (D_b + \lambda H)q_b : (D_c + \lambda H)q_c\big). \tag{10}$$

Let $A' = a_2^2$, $B' = b_2^2$, $C' = c_2^2$. Exact reduction of the barycentric distance formula gives

$$A' = \delta q_a, \qquad B' = \delta q_b, \qquad C' = \delta q_c, \qquad \delta = \frac{ABCQ^2}{H^2 q_a q_b q_c}. \tag{11}$$

The determinant of the normalized circumcevian triples gives

$$H_2^{\mathrm{or}} = -\delta Q. \tag{12}$$

Equivalently, its square follows from the factorization

$$2(q_aq_b + q_bq_c + q_cq_a) - q_a^2 - q_b^2 - q_c^2 = Q^2.$$

Finally,

$$q_a - q_b - q_c + \lambda Q = (3\lambda^2 - 1)(D_a + \lambda H), \tag{13}$$

cyclically. The first coordinate of $F_{-\lambda}^{\mathrm{or}}$ in the derived triangle is, by (11)– (12),

$$A'(A' - B' - C' - \lambda H_2^{\mathrm{or}}) = \delta^2 q_a(q_a - q_b - q_c + \lambda Q).$$

Equation (13) makes this proportional to the first coordinate in (10); the other two coordinates follow cyclically. □

The theorem contains, on the corresponding oriented ETC branches,

$$X_3 = F_0, \quad X_{61} = F_{-\sqrt{3}}, \quad X_{62} = F_{\sqrt{3}}, \quad X_{371} = F_{-1}, \quad X_{372} = F_1,$$

and the limiting member $F_\infty = X_6$. It therefore explains the circumcevian rows $X_3 \mapsto X_3$, $X_6 \mapsto X_6$, $X_{61} \mapsto X_{62}$, and $X_{371} \mapsto X_{372}$.

Let ι denote isogonal conjugation and put

$$G_\lambda = \iota(F_\lambda) = \left(\frac{1}{D_a + \lambda H} : \frac{1}{D_b + \lambda H} : \frac{1}{D_c + \lambda H}\right). \tag{14}$$

Corollary 3 (Pedal parameter law)**.** *On the same generic oriented domain,*

$$F_{-\lambda}(ABC) = G_\lambda^{\mathrm{or}}(\mathcal{T}_3(F_{-\lambda}(ABC))). \tag{15}$$

Proof. Apply Theorem 2 to $P = F_{-\lambda}$ and then apply Theorem 1. For the signed convention, let Π_P be the source power and $\mathcal{R}$ the circumradius. Determinants of the normalized derived vertex matrices give

$$\frac{H_3^{\mathrm{or}}}{H} = -\frac{\Pi_P}{4\mathcal{R}^2}, \qquad \frac{H_2^{\mathrm{or}}}{H} = -\frac{\Pi_P^3}{PA^2PB^2PC^2}.$$

The two signs agree, so the signed radicals scale by the positive square of the similarity ratio, as required. □

For the negative parameters $-\sqrt{3}$ and -1, $Q > 0$ for every nondegenerate source, so the oriented circumcevian targets above are also the positive-Heron targets. The cases $\lambda = 0$ and $\lambda = \infty$ are unchanged by sign reversal. This proves the corresponding pedal rows $X_3 \mapsto X_4$, $X_6 \mapsto X_2$, $X_{61} \mapsto X_{18}$, and $X_{371} \mapsto X_{486}$ on their stated branches.

Corollary 4 (Recovery of the classical X_{187} relations)**.** *Where the constructions are defined,*

$$M_2 : X_{187} \mapsto X_{187}, \qquad M_3 : X_{187} \mapsto X_{671}.$$

Proof. The ETC formula reduces exactly to $X_{187} = F_\lambda$ with $\lambda = S/(3H)$. From (9),

$$S_q = q_a + q_b + q_c = 6\lambda H - (3\lambda^2 + 1)S,$$

and direct subtraction gives

$$HS_q - SQ = 2(H - \lambda S)(3H\lambda - S).$$

Thus $S_q/Q = S/H$ at $\lambda = S/(3H)$. Equations (11) and (12) show that the oriented parameter of the derived triangle is $-\lambda$; after returning to the positive-Heron convention, the center is again X_{187}. The pedal result follows from Theorem 1 and the ETC identity $\iota(X_{187}) = X_{671}$. □

4.2 Branch locus and constant-family obstruction

The positive-Heron convention can hide the parameter reversal. From (12),

$$H_2^{\mathrm{or}} = -\frac{ABCQ^3}{H^2 q_a q_b q_c}. \tag{16}$$

If this quantity is negative, $F_{-\lambda}^{\mathrm{or}}$ is represented as F_λ in the positive-Heron convention, producing an apparent fixed point. If it is positive, the positive-Heron target is instead $F_{-\lambda}$.

On the regular real domain, the distance identity gives $BCH^2 q_a = -(u+v+w)^2 PA^2 < 0$ and cyclically. Hence all $q_i < 0$ and $\delta < 0$, so the sign in (16) is simply $\operatorname{sgn} Q$. Direct reduction also gives

$$u+v+w = H(\lambda S - H), \qquad Avw + Bwu + Cuv = ABCHQ.$$

The barycentric power formula therefore yields

$$\Pi_P = -\frac{ABCQ}{H(\lambda S - H)^2}. \tag{17}$$

Theorem 5 (Positive-Heron branch law)**.** *Let λ be real, with $3\lambda^2 \neq 1$, and let $P = F_\lambda(ABC)$ be an admissible finite source off the circumcircle. Where the displayed target formulas are defined,*

$$P = \begin{cases} F_{-\lambda}(\mathcal{T}_2(P)), & \Pi_P < 0, \\ F_\lambda(\mathcal{T}_2(P)), & \Pi_P > 0. \end{cases}$$

The corresponding pedal targets are $G_{-\lambda}$ and G_λ, respectively. All radicals in this statement are positive Heron radicals.

Proof. For $Q > 0$, the relative derived orientation is positive, so Theorem 2 gives the first branch. For $Q < 0$, replacing the negative derived radical by its absolute value changes $-\lambda$ to λ. Equation (17) identifies the two cases with negative and positive power. The pedal assertion follows from Theorem 1. Cancellation extends the identities at removable factors wherever the actual target remains defined. □

Thus $Q = 0$ is the circumcircle degeneracy boundary of the source. The separate locus $\lambda S = H$ concerns an infinite or undefined source. For $\lambda > 0$, the former boundary is

$$\frac{a^2+b^2+c^2}{4[ABC]} = \frac{3\lambda^2+1}{2\lambda}. \tag{18}$$

The left side has minimum $\sqrt{3}$, attained only at the equilateral shape. The right side has the same minimum at $\lambda = 1/\sqrt{3}$. Figure 2 illustrates the resulting small branch component.

The phenomenon is systematic, rather than peculiar to the nine ETC entries found by the search. At the equilateral point $A = B = C = x$, (9) reduces to

$$q_a = q_b = q_c = -(\sqrt{3}\lambda - 1)^2 x, \qquad Q = \sqrt{3}x(\sqrt{3}\lambda - 1)^2. \tag{19}$$

Consequently, for every finite real $\lambda \neq 1/\sqrt{3}$, equation (16) is positive at the equilateral limit and remains positive throughout a sufficiently small scalene neighbourhood.

Moreover, if $\lambda \neq 0$ and a generic scalene triangle satisfied $F_\lambda = F_{-\lambda}$, comparison of the first two projective coordinates would give

$$(D_a + \lambda H)(D_b - \lambda H) = (D_b + \lambda H)(D_a - \lambda H),$$

and hence $D_a = D_b$. Cyclic comparison gives $D_a = D_b = D_c$, which forces $a = b = c$. Thus in the scalene neighbourhood the positive-Heron target $F_{-\lambda}$ is genuinely different from the source F_λ.

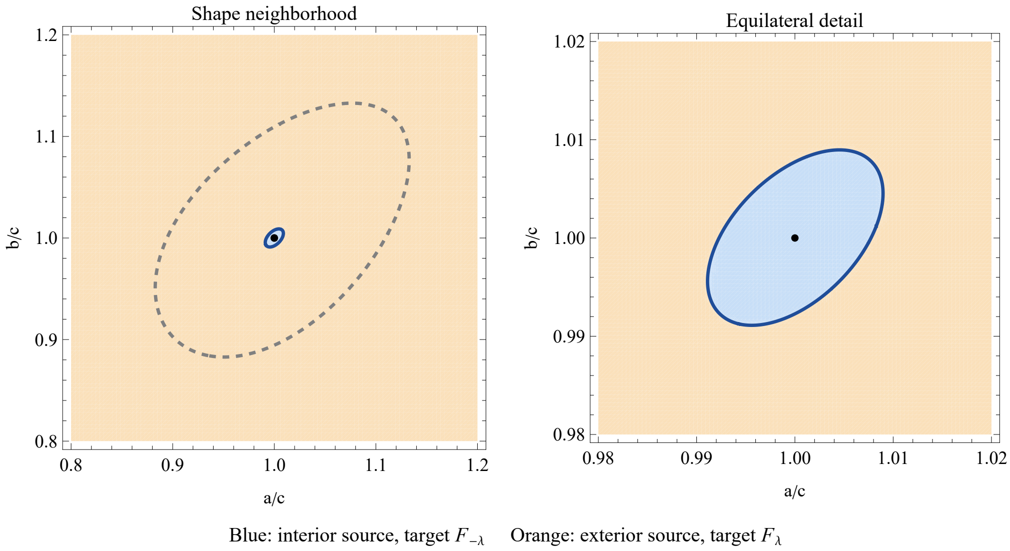

Figure 2: Positive-Heron branches for $\lambda = 4/7$ near the equilateral shape, with $c = 1$. The closed boundary is $Q = 0$; the surrounding grey curves are the excluded infinite-source locus $\lambda S = H$.

Both omitted values $\lambda = \pm 1/\sqrt{3}$ require separate treatment. Here $3\lambda^2 - 1 = 0$, so $q_a = q_b = q_c$ for every triangle on the regular part of the construction. Equation (11) makes the circumcevian triangle equilateral, while the positive-Heron formula for $F_{1/\sqrt{3}}$ on that triangle is $(0 : 0 : 0)$ and therefore defines no target center. For $F_{-1/\sqrt{3}}$ the target is the common center of this equilateral triangle, hence the circumcenter of ABC. On a scalene source $F_{-1/\sqrt{3}} \neq F_0 = X_3$, by comparison of the projective coordinates. Thus the negative parameter is not fixed either. The positive parameter has no admissible same-formula targets; such an empty domain is excluded from the meaning of a fixed-center family.

Corollary 6 (Constant-family obstruction)**.** *No finite nonzero constant member F_λ defines an unrestricted fixed-center family with nonempty admissible domain under the standard positive-Heron convention. Within the oriented parameter-reversal law, $F_0 = X_3$ is fixed, and $F_\infty = X_6$ is the corresponding limiting fixed member.*

Exact substitution in (16) is negative for $(4, 6, 7)$ but positive for the scalene near-equilateral triangle $(100000, 100001, 100002)$ for every row in Table 1. The ETC formulas in the table reduce exactly to the displayed constant F_λ. Hence all nine former fixed-point candidates fail on the near-equilateral component as immediate instances of the corollary.

Table 1: Additional M_2 fixed-point candidates rejected exactly by the near-equilateral branch test. The upper row gives the ETC index; the lower row gives λ.

6408	6454	6469	6481	10140	10144	10146	17851	17852
4/7	3/5	7/12	5/9	25/44	120/209	16/29	16/27	9/16

For example, $F_{4/7} = X_{6408}$ is classified there as $F_{-4/7} = X_{6407}$, not as X_{6408}. These parameters cluster near $1/\sqrt{3}$, where the branch boundary approaches the equilateral point; this explains why broad random tests can miss the thin component.

4.3 The fixed point X_{67371}

Theorem 7 (The X_{67371} fixed point)**.** *On the admissible domain of its polynomial barycentrics,*

$$M_2 : X_{67371} \mapsto X_{67371}$$

is an exact identity.

Proof. Write

$$\sigma_1 = A + B + C, \qquad \sigma_2 = AB + BC + CA, \qquad \sigma_3 = ABC.$$

Define

$$U = \frac{3}{2}(3A - \sigma_1)(3B - \sigma_1)(3C - \sigma_1) = \frac{3}{2}(2\sigma_1^3 - 9\sigma_1\sigma_2 + 27\sigma_3)$$

and

$$W = -\sigma_1^4 + \frac{15}{2}\sigma_1^2\sigma_2 + \frac{27}{2}\sigma_1\sigma_3 - 18\sigma_2^2.$$

If P_a is the degree-four factor multiplying $a^2 = A$ in the ETC barycentrics of X_{67371}, exact expansion gives

$$P_a = U(2A - \sigma_1) + W,$$

cyclically. Hence

$$X_{67371} = F_\Lambda, \qquad \Lambda = \frac{W}{UH}. \tag{20}$$

The mechanism is affine covariance, not a fortuitous large factorization. Put

$$k = 3\lambda^2 - 1, \qquad n = 2\lambda(H - \lambda\sigma_1).$$

Equation (9) is simply $q_i = kA_i + n$. Let U_q, W_q denote the same symmetric polynomials evaluated on (q_a, q_b, q_c). Because

$$3q_a - (q_a + q_b + q_c) = k(3A - \sigma_1),$$

and cyclically, one immediately obtains

$$U_q = k^3 U. \tag{21}$$

Substitution in the symmetric expression for W (or direct collection by degree in the translation n) gives the companion covariance

$$W_q = k^3(kW + nU). \tag{22}$$

Now set $\lambda = \Lambda = W/(UH)$. Then

$$\frac{W_q}{U_q} = k\frac{W}{U} + n = k\lambda H + n = \lambda\big((3\lambda^2 + 1)H - 2\lambda\sigma_1\big) = \lambda Q.$$

Homogeneity, together with (11) and (12), therefore gives

$$\Lambda(\mathcal{T}_2(P)) = -\frac{W_q}{U_q Q} = -\lambda.$$

Thus X_{67371} evaluated in the circumcevian triangle is precisely $F^{\mathrm{or}}_{-\lambda}$, which equals the original point by Theorem 2. The proof initially assumes $UH \neq 0$, $3\lambda^2 \neq 1$, and finite, nonzero derived formulas. Clearing denominators gives a polynomial projective identity and extends it to every admissible instance. In particular, when $U = 0$ and $W \neq 0$, the original polynomial triple is $W(A : B : C)$, so the source is X_6; this is a removable failure of the parameter representation. At $U = W = 0$ the displayed source triple is undefined, and a zero target triple is likewise excluded. $\square$

Corollary 8 (A second affine-covariant fixed center)**.** *On its admissible domain, $M_2 : X_{9181} \mapsto X_{9181}$ is exact.*

Proof. Put $\widetilde{W} = 2\sigma_1 U/3 - W$. Exact expansion of the ETC formula gives

$$X_{9181} \sim \big(A\{U(2A - \sigma_1) + \widetilde{W}\} : \cdots : \cdots\big).$$

Thus it is F_μ, with $\mu H = 2\sigma_1/3 - W/U$ wherever $U \neq 0$. Since $\sigma_{1,q} = k\sigma_1 + 3n$, the covariance identities give

$$\widetilde{W}_q = k^3(k\widetilde{W} + nU).$$

The preceding proof applies with $\widetilde{W}$ replacing W. Polynomial cancellation extends the result wherever the actual source and target are defined. □

Since $\iota(X_{67371}) = X_{54602}$ in the ETC, the transfer principle also proves $M_3 : X_{67371} \mapsto X_{54602}$. This off-diagonal corollary is outside the enumerated strips and is not included in their counts.

4.4 Elementary relations in the census

Proposition 9. *On their admissible domains,*

$$M_1 : X_2 \mapsto X_2, \qquad M_1 : X_7 \mapsto X_6, \qquad M_2 : X_1 \mapsto X_4, \qquad M_3 : X_1 \mapsto X_3.$$

Proof. For $P = (u : v : w)$, direct substitution in the normalized cevian vertices gives $P_{\mathcal{T}_1} = (v + w : w + u : u + v)$. In particular the centroid is the centroid of its medial triangle.

For the Gergonne point put $x = s - a$, $y = s - b$, $z = s - c$, so $P = (1/x : 1/y : 1/z)$. Its cevian triangle is the contact triangle. The squared side opposite the contact point on BC is $4x^2yz/((x + z)(x + y))$, cyclically, since the two tangent lengths from A are x and $\sin^2(A/2) = yz/(bc)$. These squared sides are proportional to $(1/y+1/z : 1/z+1/x : 1/x+1/y)$, proving the symmedian relation.

Finally the incenter is the circumcenter of its contact triangle, which is its pedal triangle. This proves the M_3 assertion, and the M_2 assertion follows by isogonal transfer since $\iota(X_4) = X_3$. □

5 Centroid preimages and an exact degeneracy theorem

Theorem 10 (Steiner-inellipse focus characterization; classical)**.** *Let P lie off the circumcircle and suppose its circumcevian triangle is nondegenerate. Then*

$$P \text{ is the centroid of } \mathcal{T}_2(P) \quad \Longleftrightarrow \quad P \text{ is a focus of the Steiner inellipse of } ABC.$$

Consequently,

$$M_2 : X_{39162} \mapsto X_2, \qquad M_2 : X_{39163} \mapsto X_2,$$

and, by Theorem 1,

$$M_3 : X_{39162} \mapsto X_6, \qquad M_3 : X_{39163} \mapsto X_6.$$

This equivalence belongs to the classical circumcevian class table [4]; the modern focus labels are supplied by the ETC [1]. The proof below is included because it is short, intrinsic, and independently validates the coordinate pipeline used in the census.

Proof. Normalize the circumcircle to the complex unit circle, with vertex affixes a, b, c, and let p be the affix of P, $q = \overline{p}$. The second intersection of AP with the circle is

$$a_2 = \frac{p-a}{1-qa} = p + \frac{a(pq-1)}{1-qa},$$

cyclically. Since $pq \neq 1$, the centroid condition $a_2 + b_2 + c_2 = 3p$ is equivalent to

$$\frac{a}{1-qa} + \frac{b}{1-qb} + \frac{c}{1-qc} = 0.$$

Writing

$$\Phi(q) = (1-aq)(1-bq)(1-cq) = 1 - s_1 q + s_2 q^2 - s_3 q^3,$$

this equation is $\Phi'(q) = 0$. Conjugation, using $|a| = |b| = |c| = 1$, gives

$$3p^2 - 2s_1 p + s_2 = 0.$$

This is precisely the derivative of $(z-a)(z-b)(z-c)$. The Siebeck–Marden theorem identifies its two roots with the foci of the Steiner inellipse [6, 7]. The ETC labels of these foci are X_{39162} and X_{39163}; the final two relations follow because $\iota(X_2) = X_6$. □

Together with the classical cevian and pedal cases, the nondegenerate centroid-preimage list found by the scan is therefore

$$\mathcal{C}_1(2,2), \qquad \mathcal{C}_2(39162,2), \quad \mathcal{C}_2(39163,2), \qquad \mathcal{C}_3(6,2),$$

and the circumcevian rows have the intrinsic proof just given.

Proposition 11 (The exact X_{795} degeneracy)**.** *Where its barycentric formula is finite, X_{795} lies on the circumcircle of ABC. If it differs from A, B, C, then $\mathcal{T}_2(X_{795}) = (X_{795}, X_{795}, X_{795})$. Hence the formal relation $M_2 : X_{795} \mapsto X_2$ is degenerate and inadmissible.*

Proof. Put $A_0 = a^3$, $B_0 = b^3$, $C_0 = c^3$. The ETC formula is cyclically

$$X_{795} = (f_a : f_b : f_c), \qquad f_a = \frac{a^2}{(B_0 - C_0)(A_0^2 - B_0 C_0)}.$$

This is the published factorization because $(b-c)(b^2+bc+c^2) = b^3 - c^3$ and $(a^2 - bc)(a^4 + a^2bc + b^2c^2) = a^6 - b^3c^3$. Substitution into the circumcircle equation and clearing the common denominator leaves

$$(B_0 - C_0)(A_0^2 - B_0C_0) + (C_0 - A_0)(B_0^2 - C_0A_0) + (A_0 - B_0)(C_0^2 - A_0B_0) = 0.$$

Thus $a^2 f_b f_c + b^2 f_c f_a + c^2 f_a f_b = 0$ identically. Every second intersection is therefore X_{795}, and the derived triple has zero area. □

6 Computational protocol and scope

The local formula snapshot contains 72807 consecutive ETC entries, with no index gap or symbolic expansion failure in its first-coordinate cache. Completeness of this index list is not numerical evaluability: a formula may be nonreal, infinite, undefined, or yield a degenerate derived triangle. Unavailable evaluations are neither coincidences nor counterexamples.

For each construction the enumerated region is

$$\begin{aligned} &i = j, \quad 1 \leq i \leq 72807, \\ &1 \leq i, j \leq 72807, \quad i \neq j, \quad \min(i,j) \leq 1000. \end{aligned} \tag{23}$$

The off-diagonal region consists of two directed strips, not the full square. It has

$$3\{1000(72807-1)+(72807-1000)1000\}=433839000$$

nominal comparisons per discovery triangle; the diagonal has $3\cdot 72807=218421$. The discovery triangles are the obtuse $(6,9,13)$ and the acute $(4,6,7)$.

Discovery compares normalized barycentric triples using

$$\rho(q,r)=\frac{\|q\times r\|}{\|q\|\|r\|}<10^{-9}. \tag{24}$$

This screening is followed by direct evaluation of the symbolic ETC formulas, without using the discovery fingerprints. The validation residual is the dimensionless Cartesian distance

$$\varepsilon=\frac{\|P-X_j(\mathcal{T}_k(P))\|}{\operatorname{per}(ABC)}. \tag{25}$$

The revised audit normalizes the source perimeter to one, uses 100-digit working precision, and retries insufficient-accuracy results at 180 digits. Acceptance requires $\varepsilon<10^{-40}$ and a reported absolute accuracy of at least 50 decimal digits. Degeneracy is checked using area divided by the square of the largest derived side, and finite-point normalization using the barycentric sum divided by the triple's norm; the exclusion threshold is 10^{-60}. These are numerical safeguards, not exact domain tests. An approximate zero is not an exact proof. The supplied root evaluator preserves input precision instead of truncating polynomial roots to the library's former 50 digits, while retaining its ordered-real-root convention.

The baseline contains all six labellings of

$$(4,6,7),\ (13,20,21),\ (29,30,31),\ (5,6,8),\ (4,11,13),\ (5,7,10),$$

and the 40 additional integer-sided shapes of the earlier audit (20 acute and 20 obtuse, sampled with fixed seed 20260831). Thus there are 76 labelled baseline instances, not 76 geometrically independent shapes. These are different samples evaluated with a shared formula library, not independent software implementations.

The 41 baseline survivors receive 76 further deterministic tests. For $j=2,\dots,10$, put $e=10^{-j}$ and use

$$(1,1+e,1+2e),\qquad (1,1\pm e,3/2),\qquad (1,3/2,5/2-e),$$
$$(3,4,5\pm e),\qquad (1,3/2,\sqrt{19}/2\pm e).$$

These approach equilateral, isosceles, flat, right-angle, and 120° boundaries, respectively. Four further shapes are $(100000,100001,100002)$, $(3,4,5)$, $(5,12,13)$, and $(4,13/2,15/2)$. Exact ordered inputs and individual residuals are supplied.

6.1 Correction of acute-seed coverage

The historical workers could replace an unavailable acute source by its cached coordinates on the *obtuse* discovery triangle. An exhaustive source-cache audit identifies $X_{10221},X_{66870},X_{66871}$ as incompatible fallbacks. The corrected worker preserves acute unavailability or retries the formula on the same acute triangle. Comparison of the historical 53700-entry expansion cache with the corresponding part of the expanded 72807-entry cache found no changed first-coordinate formulas.

The original search logs allow the affected comparisons to be removed without rerunning the entire search. This removes 6000 acute strip comparisons and eight acute diagonal comparisons; already-excluded instances are not subtracted again. None of the three indices occurs in the candidate union, which is therefore unchanged. Table 2 is the corrected coverage of the historical run, not a claim that full discovery was repeated with the repaired workers.

The index enumeration is exhaustive within its stated bounds, but these exclusions prevent a complete classification of even that region.

Table 2: Corrected evaluable coverage of (23).

seed	strip valid	coverage	diagonal valid	coverage
$(6, 9, 13)$	388166091	89.4724%	210351	96.3053%
$(4, 6, 7)$	388279438	89.4985%	210440	96.3460%

7 Final census and unresolved relations

The discovery union has 161 rows (113 diagonal and 48 off-diagonal). Table 3 summarizes the successive filters. The fresh audit recomputes all 161 rows on the 76 baseline instances and the 41 baseline survivors on the 76 structured instances, a total of $161 \cdot 76 + 41 \cdot 76 = 15352$ comparisons. It records 11194 passes, 2181 failures, 1976 source-unavailable instances, and one target-unavailable instance; no final record has insufficient reported accuracy.

Table 3: Filtering the discovery union. Numerical survival is not proof.

Stage	Retained rows
Union of two discovery seeds	161
Historical six-shape, 36-labelled-instance audit	54
Additional 40 shapes; confirmed by the revised baseline	41
Structured tests and exact constant-family exclusions	32
Mathematically established (20 proved here, 2 cited)	22
Still unresolved	10

Thirteen of the 54 initial survivors fail on the additional 40 shapes. They are the diagonal rows $M_1 : X_{13}$ and $M_2 : X_{13}, X_{6104}, X_{6440}, X_{6477}, X_{6522}, X_{8456}, X_{10138}, X_{10142}$, together with

$$M_2 : X_{485} \mapsto X_{61083}, \quad M_2 : X_{34321} \mapsto X_{202}, \quad M_3 : X_{13} \mapsto X_{15}, \quad M_3 : X_{485} \mapsto X_{61084}.$$

Here a diagonal row abbreviates $X_i \mapsto X_i$. These are numerical rejections; the residual files are not presented as certified interval counterexamples. Nine further diagonal rows are rejected *exactly* as unrestricted identities by Table 1; they remain valid on the outside-power branch of Theorem 5. Thus 22 of the 54 initial survivors have been eliminated as unrestricted claims.

Table 4 is the definitive retained list. Its source and target columns give ETC indices. P and C assert equality on the admissible real domain, subject to the theorem's stated qualifications; U records only the finite tests, with no established universal domain. The 20 proofs include classical recoveries and are not 20 novelty claims.

Table 4: Final retained census. P denotes a proved relation, C a cited classical relation, and U an unresolved numerical candidate. Counts give passes and unavailable instances among 152 tests; no retained row has a failing instance.

Map	Source	Target	Status / justification	Pass	Unav.
M_1	2	2	P: 9	152	0
M_1	7	6	P: 9	152	0
M_2	1	4	P: 9	152	0
M_2	3	3	P: 5	152	0
M_2	6	6	P: 5	152	0
M_2	36	186	C: [4, 3]	152	0
M_2	61	62	P: 5	152	0
M_2	187	187	P: 4	152	0

Map	Source	Target	Status / justification	Pass	Unav.
M_2	202	34321	U	152	0
M_2	203	34322	U	151	1
M_2	368	368	U	152	0
M_2	371	372	P: 5	152	0
M_2	3513	3513	U	152	0
M_2	3514	3514	U	152	0
M_2	5467	5467	U	152	0
M_2	9181	9181	P: 8	152	0
M_2	21906	21906	U	152	0
M_2	39162	2	P: 10	152	0
M_2	39163	2	P: 10	152	0
M_2	67371	67371	P: 7	152	0
M_3	1	3	P: 9	152	0
M_3	3	4	P: 5	152	0
M_3	6	2	P: 5	152	0
M_3	36	265	C: [4, 3]	152	0
M_3	61	18	P: 5	152	0
M_3	187	671	P: 4	152	0
M_3	202	6671	U	152	0
M_3	203	6672	U	152	0
M_3	371	486	P: 5	152	0
M_3	30335	175	U	152	0
M_3	39162	6	P: 10	152	0
M_3	39163	6	P: 10	152	0

For $M_2 : X_{203} \mapsto X_{34322}$ the target evaluation is unavailable at $(4, 13/2, 15/2)$; the other 151 instances pass. This is retained as an unresolved candidate, not counted as a 152-test identity or as a failure. Every other retained row passes all 152 instances.

The ten unresolved rows are not ten independent open problems. Isogonal transfer pairs $M_2 : X_{202} \mapsto X_{34321}$ with $M_3 : X_{202} \mapsto X_{6671}$, and $M_2 : X_{203} \mapsto X_{34322}$ with $M_3 : X_{203} \mapsto X_{6672}$ on common admissible domains. Likewise proved M_2 and M_3 manifestations of a single transfer relation are retained separately only to match the census convention.

Finally, angle type alone is not a branch theorem. Some rejected rows pass most acute tests but fail on another acute shape. The near-equilateral exclusions are an explicit example: the correct distinction is a circumcircle-power sign, not whether ABC is acute or obtuse. Numerical component evidence for other families must remain separate from classification by exact boundary equations.

8 Limits of the search

For $N = 72807$, testing all three maps on every ordered source-target pair would require

$$3N^2 = 15{,}902{,}577{,}747$$

comparisons on one discovery triangle. The present computation exhaustively enumerates the diagonal and the two strips in (23); it does not classify off-diagonal pairs with both indices above 1000. Moreover, the coverage in Table 2 prevents a claim of complete classification even inside the nominal strips. A full search should first develop an indexed invariant, a nearest-neighbour structure for derived fingerprints, or a family-level symbolic reduction. Before merely enlarging the quadratic source–target search, the next stage should also compare every surviving class systematically with Kimberling's central-triangle theory, Stothers's circumcevian and pedal tables, and Gibert's parameter families. That comparison is mathematically more informative than increasing the raw index bound without a structural invariant.

9 Reproducibility and logical status

The supplied supplement, version 1.1.0, fixes the ETC snapshot and provides portable programs, human-readable formulas alongside MX caches, historical discovery records, ordered test triangles, residuals, and machine-readable status tables. A SHA-256 manifest identifies every distributed file. The computations were checked using Wolfram 15.0.0 for Microsoft Windows (64-bit); the snapshot was written on 22 August 2026. Python programs use only the standard library.

The small verification workflow reruns the exact polynomial checks, the X_{795} degeneracy check, the 15352-comparison audit, the coverage correction, and the final tables without repeating discovery. The exact-check report has `allChecksTrue=true`, and all nine ETC constant-family identifications are exact. The algebraic proofs are included in the article; software checks supplement, rather than replace, their domain arguments.

The full historical discovery pipeline and its checkpoints are supplied separately from the revised verification workflow. Reproducing hundreds of millions of comparisons is optional and substantially more expensive. Appendix A describes the provenance distinction. The ten U rows in Table 4 remain computational candidates irrespective of the number of passed tests.

Acknowledgements

This problem was initially posed by Mowaffaq Hajja in unpublished work and was communicated personally to the author. Professor Hajja generously provided collected material and conjectures concerning the problem, encouraged the investigation, and granted permission for that material to be used. The author gratefully acknowledges his generosity and sustained support.

Declaration on the use of generative AI

During preparation, the author used ChatGPT and Codex, generative-AI tools developed by OpenAI, to assist in exploring arguments, drafting and testing symbolic and numerical code, interpreting computational results, editing language, and preparing LaTeX. The author accepts responsibility for the mathematical claims, computations, references, and final text. These tools are not authors or coauthors. Their assistance does not constitute independent mathematical verification.

A Supplement inventory and provenance

The supplement root contains `M1M2M3.tex`, the compiled article, its figure and generated table, and `README.md` with reproduction commands. `reproduce.py` runs the revised verification; `verify_bundle.py` verifies the manifest. The data subtree `data/LeJean-Kimberling` contains the fixed ETC snapshot, its supporting Wolfram source library, and the upstream license and attribution. Readable snapshots permit rebuilding platform-dependent MX files with the supplied conversion program.

Discovery began with first-500 and 501–1000 blocks through X_{53700}, then extended the opposite and diagonal bounds to X_{72807}. The directories `offdiagonal_first500`, `offdiagonal_501_1000`, and `unified`, under `output/m1m2m3`, retain those records. Their historical file `universal_candidates.csv` means only a six-shape audit survivor; it is superseded as a final classification by `revision_20260907/final_status.csv`.

The subdirectory `revision_20260907` contains the full source-cache audit, corrected coverage with row-level subtraction details, the fresh validation, and a status for all 161 discoveries. `algebraic_revision` contains the exact polynomial checks and nine near-equilateral branch certificates. `referee_revision` retains the earlier 40-shape experiment and the X_{795} exact check. Pre-correction source programs are retained only in `provenance_sources`, explicitly distinguished from runnable revised programs. The manifest and version identify the supplied release; no permanent-archive identifier is asserted here.

References

[1] C. Kimberling, *Encyclopedia of Triangle Centers*, University of Evansville, https://faculty.evansville.edu/ck6/encyclopedia/.

[2] C. Kimberling, Triangle centers and central triangles, *Congressus Numerantium* **129** (1998), 1–295.

[3] W. W. Stothers, *The Pedal Triangle*, University of Glasgow, https://www.maths.gla.ac.uk/wws/cabripages/triangle/ninepoint/pedal1.htm (accessed 31 August 2026).

[4] W. W. Stothers, *The Circumcevian Triangle*, University of Glasgow, https://www.maths.gla.ac.uk/wws/cabripages/triangle/ninepoint/circumcevian1.htm (accessed 31 August 2026).

[5] B. Gibert, *Table 38: Points with trilinears* $\tan(A+t)$, https://bernard-gibert.fr/Tables/table38.html (accessed 31 August 2026).

[6] M. Marden, *Geometry of Polynomials*, 2nd ed., Mathematical Surveys No. 3, American Mathematical Society, Providence, 1966.

[7] D. Kalman, An elementary proof of Marden's theorem, *Amer. Math. Monthly* **115** (2008), 330–338.